

SNUTP-98-102  
 WU-AP/73/98  
 YITP-98-64  
 hep-ph/9901436

# Gauged Monopole-Bubble

Yoonbai Kim<sup>a,1</sup>, Seung Joo Lee<sup>a,2</sup>, Kei-ichi Maeda<sup>b,3</sup>, Nobuyuki Sakai<sup>c,4</sup>

<sup>a</sup>*Department of Physics and Institute of Basic Science, Sungkyunkwan University,  
 Suwon 440-746, Korea*

<sup>b</sup>*Department of Physics, Waseda University, Tokyo 169-8555, Japan*

<sup>c</sup>*Yukawa Institute for Theoretical Physics, Kyoto University, Kyoto 606-8502, Japan*

## Abstract

The decay of a metastable false vacuum by bubble nucleation is studied in the high temperature limit of the gauge theory in which an  $SO(3)$  gauge symmetry is spontaneously broken to an  $SO(2)$ . The effects of internal symmetry are so drastic that, in addition to the known Euclidean bounce solution, there exists a new bubble solution involving a 't Hooft-Polyakov monopole at its center the moment it is nucleated. The decay rate and evolution are analyzed.

*PACS:* 11.27.+d, 03.65.Sq, 14.80.Hv

*Keywords:* Bubble; Magnetic monopole; First-order phase transition

---

<sup>1</sup>E-mail: yoonbai@cosmos.skku.ac.kr

<sup>2</sup>E-mail: suphy@newton.skku.ac.kr

<sup>3</sup>E-mail: maeda@mse.waseda.ac.jp

<sup>4</sup>E-mail: sakai@yukawa.kyoto-u.ac.jp

# 1 Introduction

Since the Euclidean bounce solution of a scalar field theory has been introduced for a description of first-order phase transition, the scalar sector of a given model determines mainly the metastable decay process [1, 2]. For cosmological phase transitions in the early universe, two more ingredients are needed to be included: one is gravitation [3] and the other may be temperature [4]. When a spontaneous continuous symmetry breaking is taken into account, an enhancement of the tunneling is expected [5]. However, the uniqueness of the bounce  $O(3)$  symmetric solution as a nucleated bubble [6] has never been doubted before three of the authors reported the global *monopole-bubble* solution in the model of a scalar triplet with global  $SO(3)$  symmetry [7, 8].

In this paper, we will address the same question to a gauge theory of  $SO(3)$  symmetry, and show that there exists another *gauged monopole-bubble* solution in which the center includes a 't Hooft-Polyakov monopole [9]. The nucleation rate of gauged monopole-bubbles is lower than that of the bounce, but it is higher than that of global monopole-bubbles. Particularly, when the mass of monopole becomes small in the strong gauged coupling limit, the decay channel through a gauged monopole-bubble with thick wall is quite considerable in the limit of high temperature. If the size of a nucleated gauged monopole-bubble is smaller than its critical size, the bubble wall starts to shrink and then the monopole at its center disappears. On the other hand, for the opposite case, the bubble wall grows and the monopole survives safely.

The remainder of this paper is organized as follows. In Sec. II we demonstrate the existence of a new gauged monopole-bubble solution in addition to the known bounce and the global monopole-bubble solution. In Sec. III we compute the nucleation rates of those solutions and present the evolution of bubbles. Section IV contains some brief concluding remarks.

## 2 Gauged Monopole-bubble Solution

The Euclidean action of Georgi-Glashow model with an  $SO(3)$  gauge symmetry is

$$S = \int_0^\beta dt_E \int d^3x \left\{ \frac{1}{4} F_{\mu\nu}^a{}^2 + \frac{1}{2} (D_\mu \phi^a)^2 + V \right\}, \quad (2.1)$$

where the field strength tensor is  $F_{\mu\nu}^a \equiv \partial_\mu A_\nu^a - \partial_\nu A_\mu^a + e\epsilon^{abc} A_\mu^b A_\nu^c$ , and the covariant derivative is  $D_\mu \phi^a \equiv \partial_\mu \phi^a + e\epsilon^{abc} A_\mu^b \phi^c$ . In order to describe a first-order phase transition, we choose a

$\phi^6$ -potential:

$$V(\phi) = \frac{\lambda}{v^2}(\phi^2 + \alpha v^2)(\phi^2 - v^2)^2, \quad (2.2)$$

where the scalar amplitude  $\phi$  is defined by  $\phi = \sqrt{\phi^a \phi^a}$  ( $a = 1, 2, 3$ ), and a parameter  $\alpha$  ( $0 < \alpha < 1/2$ ) governs the transition rate from the symmetric false vacuum at  $\phi = 0$  to a broken true vacuum at  $\phi = v$ .

In the high temperature limit, i.e.,  $\beta \rightarrow 0$ , a static electrically-neutral object satisfies

$$(D_i^2 \phi)^a = \frac{\partial V}{\partial \phi^a}, \quad (2.3)$$

$$(D_j F_{ij})^a = e \epsilon_{abc} \phi^b (D_i \phi)^c. \quad (2.4)$$

The ordinary bounce configuration is obtained under the ansatz of the scalar field  $\phi^a = (0, 0, f(r))$  with boundary conditions,  $df/dr|_{r=0} = 0$  and  $f(r = \infty) = 0$ . Here one may ask a question whether or not the gauge field affects the bounce configuration. Since the  $SO(3)$  gauge symmetry is spontaneously broken to an  $SO(2)$  symmetry and the first two components of the scalar field vanish, the gauge field decouples from the bounce solution. Therefore, even under a general ansatz for the electrically-neutral gauge field [10], it is easy to show decoupling of the gauge field from the bounce solution [11].

In this paper we are interested in a different bubble solution which is obtainable under the hedgehog ansatz:

$$\phi^a = \hat{r}^a \phi(r), \quad A_i^a = \epsilon^{aij} \hat{r}^j \frac{1 - K(r)}{er}. \quad (2.5)$$

Substituting Eq. (2.5) into Eqs. (2.3) and (2.4), we have

$$\frac{d^2 \phi}{dr^2} + \frac{2}{r} \frac{d\phi}{dr} - 2 \frac{K^2}{r^2} \phi = \frac{dV}{d\phi}, \quad (2.6)$$

$$\frac{d^2 K}{dr^2} = K \left( \frac{K^2 - 1}{r^2} + e^2 \phi^2 \right). \quad (2.7)$$

Note that the ordinary bounce solution  $\phi_b^a$  corresponds to  $K = 0$  solution where a Dirac monopole in Eq. (2.5) decouples from this solution [1], and that the global monopole-bubble  $\phi_{\text{gm}}^a$  is supported by the replacement from  $K(r)^2$  in Eq. (2.6) to 1 only when the gauge coupling  $e$  vanishes because of Eq. (2.7) [7, 8]. The first-order transition from a symmetric

false vacuum ( $\phi = 0$ ) to a true broken vacuum ( $\phi = v$ ) when  $0 < \alpha < 1/2$ ; possible boundary conditions are read as follows: regularity of the fields at the origin gives

$$\phi(r=0) = 0, \quad K(r=0) = 1, \quad (2.8)$$

and the spatial infinity should be in the initial setting before transition:

$$\phi(r \rightarrow \infty) = 0, \quad K(r \rightarrow \infty) = 1. \quad (2.9)$$

Of course, the trivial solution of false symmetric vacuum, i.e.,  $\phi = 0$  and  $K = 1$ , is an unwanted one. Therefore, as shown in Fig. 1, the nontrivial bubble solution of our interest is:  $\phi(r)$  increases from  $\phi = 0$  at the beginning, reaches a maximum value  $\phi_{\max}$ , and decreases to 0 as  $r$  goes to infinity. On the other hand,  $K(r)$  starts to decrease from 1, arrives at a minimum, and then grows up to 1 at spatial infinity.

To read the physics of the obtained sphaleron-type monopole-bubble solution, let us examine energy density:

$$T_0^0 = \frac{1}{e^2 r^2} \left[ \left( \frac{dK}{dr} \right)^2 + \frac{(K^2 - 1)^2}{2r^2} \right] + \frac{1}{2} \left( \frac{d\phi}{dr} \right)^2 + \frac{K^2}{r^2} \phi^2 + V. \quad (2.10)$$

For small  $r$  we attempt a power series solution:

$$\phi(r) \approx \phi_0 \left[ r - \frac{1}{10} (4\kappa_0 - m^2) r^3 + \dots \right], \quad (2.11)$$

which is formally odd under  $r \rightarrow -r$ , and

$$K(r) \approx 1 - \kappa_0 r^2 + \frac{1}{10} (3\kappa_0^2 + e^2 \phi_0^2) r^4 + \dots, \quad (2.12)$$

which is even in form under  $r \rightarrow -r$ . Here  $m$  denotes the mass of scalar particles at the symmetric vacuum, i.e.,  $m = \sqrt{d^2 V / d\phi^2|_{\phi=0}} = \sqrt{2\lambda(1-2\alpha)}v$ . If  $\kappa_0$  is negative, then Eq. (2.7) says that  $K(r)$  is a monotonic increasing function bounded below 1. It means that any solution with a negative  $\kappa_0$  cannot satisfy the boundary condition (2.9) at spatial infinity, and thereby  $\kappa_0$  must be positive. A characteristic of this new monopole-bubble, which makes it distinguished from the ordinary bounce configuration, is to have a matter lump at the center of the bubble. If we look into the behavior of energy density for small  $r$  by use of the formulas (2.11) and (2.12), it has

$$T_0^0 = 6\kappa_0^2 e^2 + \frac{3\phi_0^2}{2} + \lambda \alpha v^4 + \left[ m^2 \phi_0^2 - 2\kappa_0 \left( \frac{4\kappa_0^2}{e^2} + 3\phi_0^2 \right) \right] r^2 + \dots \quad (2.13)$$

The first term in Eq. (2.13) is always positive, which stems from the winding between the 3-dimensional space and the SO(3) internal space. It is an evidence of the formation of an

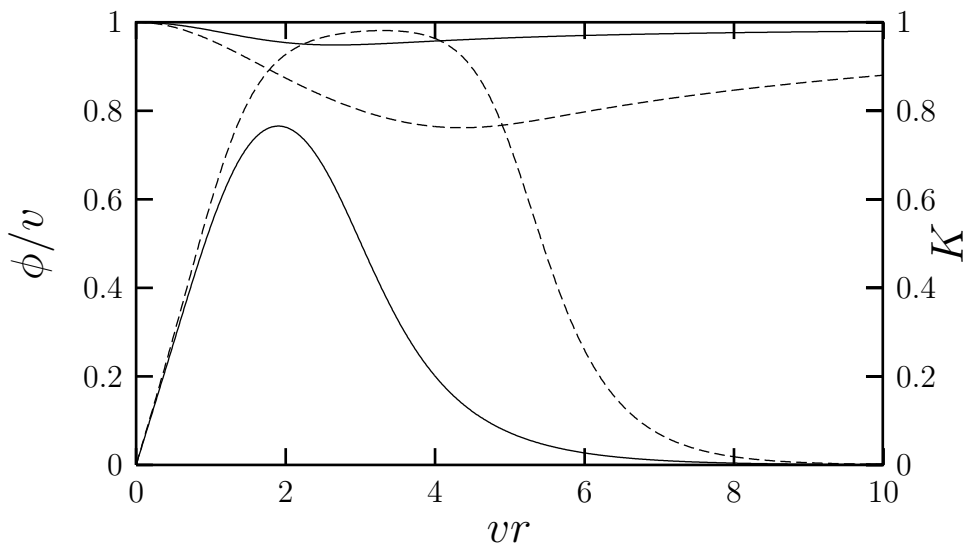


Figure 1: Plots of monopole-bubbles for  $\lambda = 1$  and  $e = 0.3$ . The dashed lines correspond to the scalar amplitude  $\phi(r)/v$  and the gauge field  $K(r)$  of a thin-wall monopole-bubble ( $\alpha = 0.15$ ), and the solid lines to those of a thick-wall monopole-bubble ( $\alpha = 0.35$ ).

extended object at the center of the bubble. The behavior of energy density at the center depends on the sign of the second term in Eq. (2.13). If it is positive,  $T_0^0(r)$  increases from 0, reaches a maximum, and decreases, as shown in the solid line of Fig. 2. This structure is like a domain wall with the width  $1/m_H \sim 1/\sqrt{8\lambda(1+\alpha)}v$ . In the case of global monopole-bubbles, the existence of this wall is automatic since  $\kappa_0$  is zero and the second term is always positive [7, 8]. However, when the gauge coupling is sufficiently large so as to make the second term negative, strong gauge repulsion can sweep the monopole wall away and the energy density is a decreasing function near the origin, as shown in the dashed line of Fig. 2.

At the asymptotic region for large  $r$ , the scalar field approaches the boundary value in Eq. (2.9) exponentially,

$$\phi \approx \phi_\infty \frac{1 + mr}{(mr)^2} e^{-mr}. \quad (2.14)$$

The gauge field has a long range power tail because the gauge boson becomes massless in the symmetric phase,

$$K(r) \approx 1 - \frac{\kappa_\infty}{r} + \frac{3\kappa_\infty^2}{4r^2} + \dots, \quad (2.15)$$

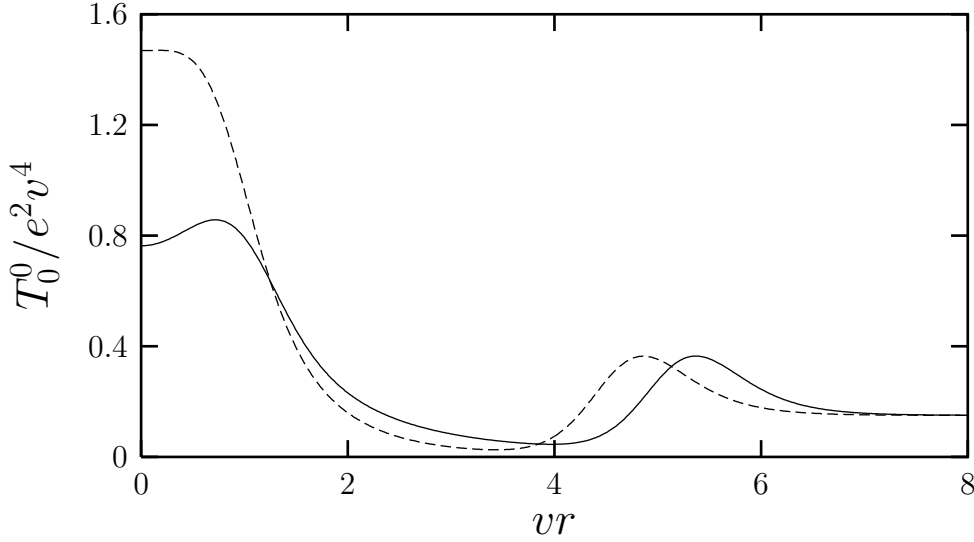


Figure 2: Profiles of the energy density for  $\lambda = 1$  and  $\alpha = 0.35$ . The solid line stands for a monopole-bubble with a monopole wall ( $e = 0.1$ ), and the dashed line for a monopole-bubble without a monopole wall ( $e = 0.65$ ).

where  $\kappa_\infty$  should also be nonnegative for the same reason as  $\kappa_0$  is in Eq. (2.12). Outside the bubble wall, the vacuum is in the symmetric phase with  $\langle \phi \rangle = 0$ , and the  $\text{SO}(3)$  gauge field is massless. Specifically, the magnetic field looks like that of a dipole:

$$F_{ij}^a \sim \frac{1}{e} (\epsilon^{ajk} \hat{r}^i - \epsilon^{aik} \hat{r}^j) \frac{\hat{r}^k}{r} \frac{dK}{dr} \sim \mathcal{O}(1/r^3). \quad (2.16)$$

The corresponding leading term of the energy density,  $T_0^0 - V(0)$ , in Eq. (2.10) is of order  $1/r^6$ , and this fast decay can also be read from Fig. 2. This means that the monopole at the center is screened by the bubble wall.

In the remainder of this section we make analytic arguments on the properties of gauged monopole-bubbles under the thin-wall assumption. If the energy gap between the false vacuum and the true vacuum,  $\Delta V \equiv V(0) - V(v) = \lambda \alpha v^4$ , is small enough, the bubble radius becomes much larger than both of the monopole size and the width of bubble wall, and we may adopt the thin-wall approximation. The typical scale of the monopole core or the outer wall is given  $\sim 1/m_H$  by the configuration of the Higgs field, while it is given  $\sim 1/ev$  by the configuration of the gauge field. Here we assume that both scales are much smaller than the bubble radius, and therefore we implicitly exclude the weak coupling case  $e \ll 1$ . First, let us consider the behavior of the fields near the maximum scalar amplitude

$\phi_{\max}$ , which is close to  $v$  (see the solid lines in Fig. 1). Around  $\phi = \phi_{\max}$ , the derivative of the scalar field  $d\phi/dr$  is close to zero, and the slope of the potential  $dV/d\phi$  is almost flat. Therefore, if the corresponding value of  $K$  at the turning point  $r_{\text{turn}}$  with  $\phi(r_{\text{turn}}) = \phi_{\max}$  is negligibly small, which will turn out to be indeed the case, the scalar field equation (2.6) implies that the quadratic derivative of the potential  $d^2V/d\phi^2$  is also very small near  $\phi_{\max}$ . Thus we see that  $\phi$  stays near  $\phi_{\max}$  for a long range of  $r$ . In this case, the first term of the right-hand side of Eq. (2.7) becomes negligible near  $\phi \approx \phi_{\max}$  since  $r_{\text{turn}}$  is large enough. Therefore,  $K$  falls to zero exponentially, i.e.,  $K \sim e^{-e\phi_{\max}r}$ , where the scale  $e\phi_{\max} \approx ev$  in the exponential is nothing but the mass of gauge boson in the Higgs phase. We can also confirm that  $\phi$  approaches exponentially to the true vacuum expectation value  $v$ , i.e.,  $\phi \approx v - \phi_{\max}e^{-m_H r}/m_H r$  where  $\phi_{\text{turn}}$  is a constant to be fixed by boundary conditions (2.8) and (2.9).

Secondly, we discuss how energy density is distributed in the region between the monopole core and the bubble wall. Because this region is in a symmetry-broken phase of which the breaking pattern is  $\text{SO}(3) \rightarrow \text{SO}(2)$ , one of the three internal gauge degrees remains massless and it is to be identified as the photon field described by

$$F_{\mu\nu} = \frac{\phi^a}{\phi} F_{\mu\nu}^a + \frac{1}{e\phi^3} \epsilon_{abc} \phi^a (D_\mu \phi)^b (D_\nu \phi)^c. \quad (2.17)$$

Inserting the monopole ansatz (2.5) into Eq. (2.17), we obtain zero electric field but in contrast the magnetic field with the monopole charge  $g = 1/e$ , i.e.,  $F_{ij} = \epsilon^{ija} \hat{r}^a / er^2$ . Since  $\phi \approx v$  and  $K \approx 0$  around  $r = r_{\text{turn}}$ , one can easily notice that the contribution of the magnetic field comes from the first term of Eq. (2.17), and then identify the matter lump produced at the center as a 't Hooft-Polyakov monopole [9]. If we look at the expression of energy density (2.10) near  $\phi = \phi_{\max} \sim v$ ,

$$T_0^0 \sim \frac{1}{2e^2 r^4} + V(v), \quad (2.18)$$

the above leading term is interpreted as magnetic energy of a 't Hooft-Polyakov monopole, and its total energy is finite when we do not take into account the contribution from latent heat term  $V(v)$ . This is different from the global monopole-bubble case, where the produced global monopole contributes a  $1/r^2$  term to energy density, since this scalar phase term, which would make the energy diverge, is eaten up by the gauge field.

Finally, we argue how the gauge field affects the bubble size. Let us estimate the radius by Coleman's action-minimum method [1, 13]. After assuming spherical symmetry and the

hedgehog configuration (2.5), the action (2.1) is reduced to

$$S = 4\pi\beta \int_0^\infty r^2 dr \left\{ \frac{1}{2} \phi'^2 + \frac{K^2 \phi^2}{r^2} + V + \frac{(1 - K^2)^2}{2e^2 r^4} + \frac{K'^2}{e^2 r^2} \right\}. \quad (2.19)$$

By the thin-wall assumption, the core is approximately described as a 't Hooft-Polyakov monopole, and we may approximate  $\phi = v$  and  $K = 0$  between the monopole core and the bubble wall. Then the difference between the action for a gauged monopole-bubble and that for the false vacuum is

$$\begin{aligned} B_{\text{lm}} &\equiv S(\phi) - S(\phi = 0) \\ &= \beta \left( -\frac{4\pi}{3} R^3 \Delta V + 4\pi\sigma_\phi R^2 + M_K - \frac{2\pi}{e^2 R} \right) + \text{constant core term}, \end{aligned} \quad (2.20)$$

where  $R$  is the bubble radius, and  $\sigma_\phi$  and  $M_L$  are constants, which are defined as

$$\sigma \equiv \frac{1}{2} \int_{R-\epsilon}^{R+\epsilon} dr \left( \frac{d\phi}{dr} \right)^2, \quad M_K \equiv \frac{4\pi}{e^2} \int_{R-\epsilon}^{R+\epsilon} dr \left( \frac{dK}{dr} \right)^2 t. \quad (2.21)$$

Similarly, for a normal bubble and a global monopole-bubble, we obtain

$$B_{\text{b}} = \beta \left( -\frac{4\pi}{3} R^3 \Delta V + 4\pi\sigma_\phi R^2 \right), \quad (2.22)$$

$$B_{\text{gm}} = \beta \left( -\frac{4\pi}{3} R^3 \Delta V + 4\pi\sigma_\phi R^2 + 4\pi v^2 R \right) + \text{constant core term}. \quad (2.23)$$

Each radius is determined by the condition  $dB/dR = 0$ :

$$R_{\text{b}} = \frac{2\sigma_\phi}{\Delta V}, \quad R_{\text{gm}} \approx R_{\text{b}} + \frac{v^2}{2\sigma_\phi} \quad (2.24)$$

What we need is an inequality among  $R_{\text{b}}$ ,  $R_{\text{gm}}$ ,  $R_{\text{lm}}$  rather than a complicated expression of  $R_{\text{lm}}$ . Thus we evaluate

$$\left. \frac{dB_{\text{lm}}}{dR} \right|_{R=R_{\text{b}}} = \frac{2\pi\beta}{e^2 R_{\text{b}}^2} > 0, \quad \left. \frac{dB_{\text{lm}}}{dR} \right|_{R=R_{\text{gm}}} = 2\pi\beta \left( \frac{1}{4e^2 R_{\text{gm}}^2} - v^2 \right) < 0, \quad (2.25)$$

where the last inequality is supported by the initial assumption  $R \gg 1/ev$ . Because  $R_{\text{lm}}$  is a local maximum of  $B_{\text{lm}}$ , Eq. (2.25) imply

$$R_{\text{b}} < R_{\text{lm}} < R_{\text{gm}}. \quad (2.26)$$

We may interpret that the bubble radius is mostly determined by energy inside the bubble.



### 3 Nucleation Rate and Evolution

We begin this section by comparing the nucleation rates of the bounce and of gauged monopole-bubbles. In the semiclassical approximation, the decay rate per unit volume is estimated by the use of the leading exponential factor which is given by the Euclidean action of the bubble solution [1], multiplied by a prefactor determined by zero modes of the fluctuation [2]. When a continuous symmetry or a part of it is spontaneously broken, the number of zero modes increases and then the tunneling rate into vacua is enhanced [5]. In the present model, the  $SO(3)$  gauge symmetry is broken to an  $SO(2)$  symmetry and we have two bubble solutions; the relative decay rate between the bounce  $\phi_b^a$  and the gauged monopole-bubble  $\phi_{lm}^a$  is meaningful:

$$\frac{\Gamma_{lm}}{\Gamma_b} \sim \left( \frac{S(\phi_{lm}^a)}{S(\phi_b^a)} \right)^{3/2} \left| \frac{\det'[S''(\phi_{lm}^a)]}{\det'[S''(\phi_b^a)]} \right|^{-1/2} \frac{\int d^3x (\phi_{lm}^a)^2}{\int d^3x (\phi_b^a)^2} e^{-[S(\phi_{lm}^a) - S(\phi_b^a)]}, \quad (3.27)$$

where primed determinants denote infinite products over the nonzero eigenvalues, which are assumed to be order 1 here. The value of the action in Eq. (3.27) is estimated after removing the constant vacuum energy density at the metastable symmetric vacuum, that means  $S(\phi = 0) = 0$  in Eq. (3.27).

In order to see the leading effect, we plot in Fig. 3 the values of the Euclidean actions for a bounce, gauged monopole-bubbles ( $e = 0.3$  and  $0.91$ ), and global monopole-bubble for  $e = 0$ . As expected, the bounce has always the minimum action irrespective of the thickness of the bubble wall (or equivalently the parameter  $\alpha$ ) (see Fig. 3) so that it forms a dominant decay channel (see Table 1). The difference of the Euclidean actions is almost a constant for a given gauge coupling  $e$ , and it is roughly the monopole mass multiplied by inverse temperature. The values of the Euclidean action decrease as the gauge coupling increases. If we recall the mass formula  $4\pi v/e$  of BPS monopole of unit winding [12], one may easily notice that this gap decreases in the strong coupling limit. This behavior can easily be understood by rescaling the variables to the dimensionless ones:  $\tilde{t}_E = evt_E$ ,  $\rho = evr$ ,  $\phi = vh$ ,  $\tilde{V} = \tilde{\lambda}(h^2 + \alpha)(h^2 - 1)^2$ , and  $\tilde{\lambda} = \lambda/e^2$ . Then the action is rewritten as  $S \sim (4\pi v\beta/e) \times (\text{dimensionless energy})$ , which reflects the decrease of the monopole mass for strong gauge coupling. If we take into account the enhancement due to the prefactor in Eq. (3.27), we may obtain even an unbelievable relative decay rate in the high temperature limit, e.g.,  $\Gamma_m/\Gamma_b > 1$  when  $v\beta = 0.1$  and  $\alpha = 0.4$ . However, since the transition pattern becomes weakly first-order at such high temperature, the above result does not imply a possibility that the decay through a monopole-bubble is dominant decay channel. Instead, it means that in a high temperature ( $v\beta \sim 1$ ) the relative production rate is considerable for thick-wall bubbles ( $\alpha \approx 0.4$ ) with strong gauge

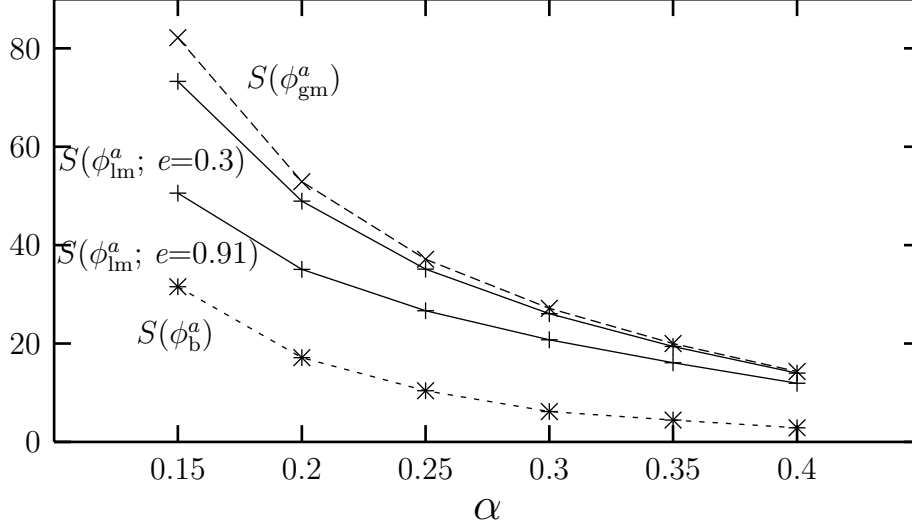


Figure 3: Plots of Euclidean actions  $S/v\beta$  versus  $\alpha$  for various bubble solutions. The dashed line corresponds to a global monopole-bubble ( $e = 0$ ), two solid lines to gauged monopole-bubbles of  $e = 0.3$  and  $0.91$ , and the dotted line to an ordinary bounce. Here  $\lambda$  is set to be 1.

coupling ( $e \sim 1$ ) (see Table 1). For reference we give the values of the Euclidean action for the global monopole-bubbles when  $e = 0$ , which are always larger than those of the gauged monopole-bubbles because of their long energy tail proportional to the radius of the global monopole-bubble.

Completion of the first-order phase transition is achieved by the growth and percolation of nucleated bubbles. The actual process is complicated because our  $O(3)$  bounces and gauged monopole-bubbles are generated at high temperature. However, one simple but probably correct way is to analyze the time-dependent field equations with appropriate initial configurations. The obtained Euclidean solution is time-independent both in Euclidean spacetime and in Lorentzian spacetime, and it therefore does not evolve in itself. Hence we give small radial fluctuations to the static solution as an initial configuration, and solve the time-dependent field equations numerically. If the bubble radius is smaller than the critical radius, both the bounce and the gauged monopole-bubble collapse; so does the magnetic monopole at its center. On the other hand, as Fig. 4 shows, if it is larger than the critical radius, the bubble wall starts to grow and the magnetic monopole remains to be stable with small damped oscillation. The thick wall of the monopole-bubble becomes a thin wall. We

$\alpha$	0.2	0.3	0.4
$(\Gamma_{\text{gm}}/\Gamma_{\text{b}}) _{e=0}$	$1 \times 10^{-15}$	$6 \times 10^{-9}$	$1 \times 10^{-4}$
$(\Gamma_{\text{lm}}/\Gamma_{\text{b}}) _{e=0.3}$	$6 \times 10^{-14}$	$2 \times 10^{-8}$	$1 \times 10^{-4}$
$(\Gamma_{\text{lm}}/\Gamma_{\text{b}}) _{e=0.91}$	$4 \times 10^{-8}$	$2 \times 10^{-6}$	$8 \times 10^{-4}$

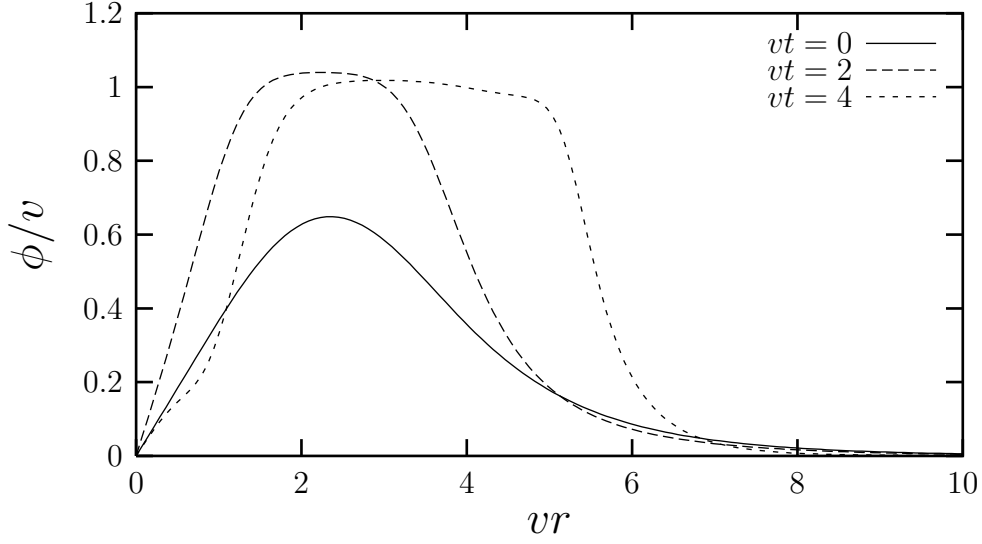
Table 1: The values of the relative decay rates,  $\Gamma_{\text{gm}}/\Gamma_{\text{b}}$  and  $\Gamma_{\text{lm}}/\Gamma_{\text{b}}$ , for various  $\alpha$  and  $v\beta$  with  $e = 1$ ,  $\lambda = 1$ , and  $v\beta = 1$  when we set the ratio of determinant factors to be 1.

also find the the velocity of the wall approaches the light velocity. Of course, inclusion of radiation is needed to obtain the bubble dynamics more precisely. Here we just give a short comment on this topic: since we have three massless gauge bosons outside the bubble wall and only one photon inside it, the expected pressure difference may decrease the terminal velocity of the wall.

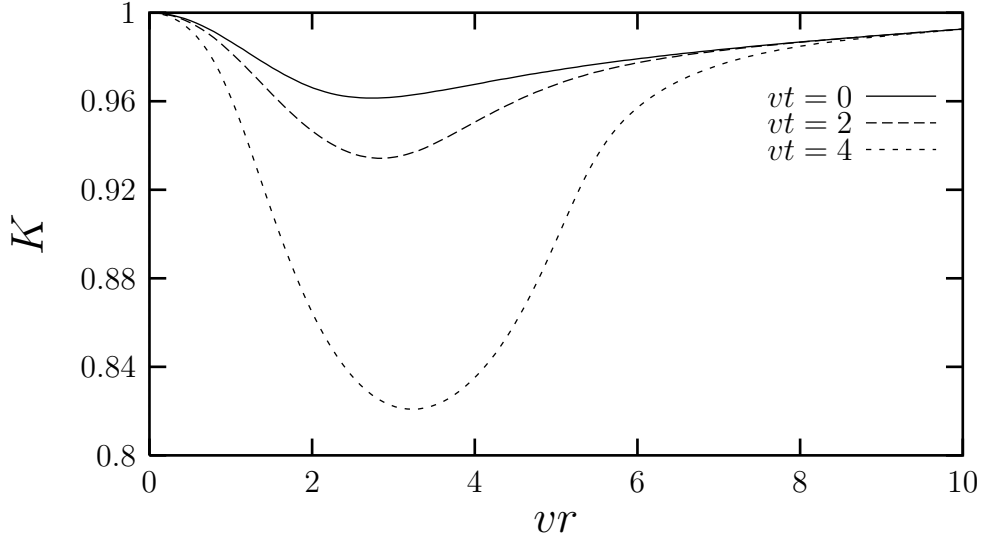
## 4 Concluding Remarks

We have seen that when a first-order phase transition in the gauge theory in which the symmetry breaking pattern is  $\text{SO}(3) \rightarrow \text{SO}(2)$  is considered in the high temperature limit; a new gauged monopole-bubble solution was found. It is distinguished from the known Euclidean bounce by the production of a 't Hooft-Polyakov monopole at the center of the bubble the moment it is nucleated. The production rate of monopole-bubbles is smaller than that of the bounce, but it is considerable for thick-wall cases with strong gauge coupling in the limit of high temperature. When the size of a nucleated bubble is larger than the critical size, the bubble wall starts to move outward so that the magnetic monopole remains stable in the bubble at least before bubble collision.

In a theoretical sense, the existence of such a gauged monopole-bubble solution demonstrates clearly a possible drastic effect of the gauge field on bubble nucleation. Although it is important to understand the evolution of the gauged monopole-bubble through zero-modes, the stability including angular fluctuations is left for future work. The realization of these monopole-bubbles in a real material is not known yet.



(a)



(b)

Figure 4: Evolution of a gauged monopole-bubble with a thick-wall: (a) scalar amplitude  $\phi/v$  and (b) gauge field  $K$ , where  $\lambda = 1$ ,  $e = 0.3$ , and  $\alpha = 0.4$ .

## Acknowledgments

The authors would like to thank Kyoungtae Kimm for discussions. Numerical Computation of this work was carried out at the Yukawa Institute Computer Facility. Y.K. wishes to acknowledge the financial support of the Korea Research Foundation made in the program year of 1997. N. S. was supported by JSPS Research Fellowships for Young Scientist. This work was supported partially by the Grant-in-Aid for Scientific Research Fund of the Ministry of Education, Science, Sports and Culture (No. 9702603 and No. 09740334) and by the Waseda University Grant for Special Research Projects.

## References

- [1] S. Coleman, Phys. Rev. D 15 (1977) 2929; M. B. Voloshin, I. Yu. Kobzarev, and L. B. Okun, Yad. Fiz. 20 (1974) 1229; P. H. Frampton, Phys. Rev. D 15 (1977) 2922.
- [2] C. Callan and S. Coleman, Phys. Rev. D 16 (1977) 1762.
- [3] S. Coleman and F. De Luccia, Phys. Rev. D 21 (1980) 3305.
- [4] A. D. Linde, Phys. Rev. B 100 (1981) 37; Nucl. Phys. B 216 (1983) 421.
- [5] A. Kusenko, Phys. Lett. B 358 (1995) 47; A. Kusenko, K. Lee, and E. J. Weinberg, Phys. Rev. D 55 (1997) 4903.
- [6] S. Coleman, Nucl. Phys. B 298 (1988) 178.
- [7] Y. Kim, Nagoya university preprint DPNU-94-39, hep-th/9410076 (unpublished).
- [8] Y. Kim, K. Maeda, and N. Sakai, Nucl. Phys. B 481 (1996) 453.
- [9] G. 't Hooft, Nucl. Phys. B 79 (1974) 276; A. M. Polyakov, Zh. Eksp. Teor. Fiz. Pis'ma Red. 20 (1974) 43 (JETP Lett. 20 (1974) 194).
- [10] E. Witten, Phys. Rev. Lett. 38 (1977) 121.
- [11] Y. Kim, K. Kimm, K. Maeda, N. Sakai, in preparation.
- [12] E. B. Bogomol'nyi, Sov. J. Nucl. Phys. 24 (1976) 449; M. K. Prasad and C. M. Sommerfield, Phys. Rev. Lett. 35 (1975) 760.
- [13] A.D. Linde, *Particle Physics and Cosmology* (Harwood, 1990).